Research Article

Ecological causes of speciation and species richness in the mammal tree of life

Short title: Ecological causes of mammal diversity

Nathan S. Upham[1*], Jacob A. Esselstyn[2], and Walter Jetz[3]

Author affiliations:

[1]Department of Ecology & Evolutionary Biology, Yale University, New Haven, CT 06511 USA, nathan.upham@yale.edu. [2]Department of Biological Sciences and Museum of Natural Science, Louisiana State University, Baton Rouge, LA 70803 USA, esselstyn@lsu.edu. [3]Department of Ecology & Evolutionary Biology, Yale University, New Haven, CT 06511 USA, walter.jetz@yale.edu.

*Corresponding author:

165 Prospect St., OML 122, New Haven, CT 06511 USA, nathan.upham@yale.edu.

Keywords:

Phylogenetics, macroevolution, trait-associated diversification, dispersal, latitude, diel activity

Abstract: 150 words; Main text: 4,620 words; 88 references, 5 figures

ABSTRACT

Biodiversity is distributed unevenly from the poles to the equator, and among branches of the tree of life, yet how those patterns are related is unclear. We investigated global speciation-rate variation across crown Mammalia using a novel time-scaled phylogeny (*N*=5,911 species, ~70% with DNA), finding that trait- and latitude-associated speciation has caused uneven species richness among groups. We identify 24 branch-specific shifts in net diversification rates linked to ecological traits. Using time-slices to define clades, we show that speciation rates are a stronger predictor of clade richness than age. Mammals that are low dispersal or diurnal diversify the fastest, indicating roles for geographic and ecological speciation, respectively. Speciation is slower in tropical than extra-tropical lineages, consistent with evidence that longer tropical species durations underpin the latitudinal diversity gradient. These findings juxtapose modes of lineage diversification that are alternatively turnover-based, and thus non-adaptive, or persistence-based as associated with resource adaptations.

INTRODUCTION

Biological diversity is concentrated at the equator more than the poles, and in some evolutionary lineages more than others. Yet how these organic phenomena are connected is an open question. The latitudinal diversity gradient is generally attributed to stable tropical productivity (*1–5*), but there is far less consensus regarding why species richness is distributed unevenly across the tree of life. Phylogenetic tree shape was first characterized taxonomically as species-per-genus 'hollow curves' (*6*) and later formalized under the concept of tree imbalance or unevenness (*7*). To arise, more speciose clades must have been derived from faster rates of net diversification (speciation – extinction), older ages (earlier divergences), or both. However, the relative contribution of clade rates and ages to species richness is widely disputed (e.g., (*8–11*)). Similarly controversial are the causes of diversification-rate variation in real phylogenies, whether due to stochasticity, determinism via ecological factors or time, or artifacts from how we reconstruct evolutionary history (*12–21*). Latitude might determine the rates at which new species originate and persist or go extinct (*2*, *3*, *22*, *23*), but so too might species' intrinsic traits (*24*), some of which are correlated with latitude (e.g., (*25*)). Thus, understanding the causal underpinnings of uneven species richness patterns requires connecting levels of indirect (e.g., eco-geography) and direct (e.g., rates, ages) causes to assess their joint influences. Furthermore, investigating rate variation across large swaths of the tree of life simultaneously avoids ascertainment biases and methodological differences in compendia of smaller trees (*26*).

The last ~180-million-years of crown mammalian evolution have resulted in ~6000 living species (*27*, *28*), which inhabit nearly all terrestrial biomes plus the open oceans, and thousands of preserved ancestors described as fossil taxa (*29–31*). Within this context, similarly aged clades in the mammal tree range from mega-diverse rodents (~2500 living species) and bats (~1300 species) to species-poor groups like treeshrews (20 species) and pangolins (8 species; all four share stem ages of ~60-70 million years ago [Ma] (*28*, *32*)). The early availability of a species-level 'supertree' phylogeny of mammals (now cited over 1,800 times; (*33*)) encouraged initial studies of macroevolutionary-rate covariates (e.g., (*19*, *34–36*)). However, because that pioneering supertree was assembled from hundreds of overlapping source trees, over 50% of its nodes were initially unresolved and then simulated to obtain a bifurcating time-scaled phylogeny (*33*, *37*). Timings of diversification from this supertree, along with two other mammal supertrees

75 (*11*, *38*), were consequently shown to have inflated precision relative to the large gaps in
76 available fossil age and DNA sequence data (*28*).
77 Here, we draw upon a new species-level, time-calibrated phylogeny for global
78 Mammalia, which is built from a contiguous DNA supermatrix (31 genes by 4,098 species) and
79 consists of credible sets of 10,000 trees (*28*). We used these phylogenies, which jointly model
80 topological and age uncertainty, to better understand the temporal dynamics of mammalian
81 diversification relative to the potentially causal effects of organismal and environmental factors.
82 Our objectives were three-fold. We first tested for tree-wide and branch-specific rate variation in
83 relation to geological events such as the Cretaceous-Paleogene (K-Pg) mass extinction to explore
84 whether significant shifts in net diversification rates were mutually triggered. We then use
85 neutrally defined (time-slice based) clades to explore the relative roles of clade ages and
86 speciation rates in explaining current-day species richness. Finally, we develop the link between
87 observed variation in speciation rates and its putative ecological causes, testing whether factors
88 predicted to cause newly formed species to persist or go extinct are, in turn, causing the observed
89 patterns of uneven species richness.
90 We focus on three potential ecological causes (vagility, latitude, and diurnality) of rate
91 variation. First, we tested whether low-vagility species have higher speciation rates than more
92 dispersive species, due to their greater capacity to form nascent allopatric species (*39*, *40*). For
93 this test, we developed an index of organismal vagility for all mammals (i.e., dispersal ability;
94 (*41*)). Vagility has never been assessed across mammals, although evidence in birds using the
95 hand-wing index supports an inverse vagility-to-speciation rate relationship (e.g., (*42*, *43*)).
96 Second, if unstable environments increase species ephemerality via greater lineage turnover (*44*),
97 then we expect to find higher rates of recent species-specific (i.e., 'tip') speciation in temperate
98 latitudes where climates were historically less stable (*23*, *45*). To our knowledge, no latitudinal
99 tests of tip rates have been conducted in mammals to date, but clade-level comparisons have
100 either been inconclusive (*46*) or tentatively supported greater temperate than tropical lineage
101 turnover (*22*, *36*, *47*). Lastly, we test whether diurnality (daytime activity) has increased
102 speciation rates relative to nocturnal clades, following recent evidence that all mammals were
103 nocturnal until daytime niches evolved ~35 Ma (*48*, *49*). The influence of diurnality on
104 speciation rates has thus far only been investigated in primates (*50*), although a mammal-wide
105 study did investigate ancestral activity states (*49*). We are thus using species-level trait proxies to

106 investigate scenarios of geographic, ephemeral, and adaptive modes of species diversification in
107 mammals, respectively.
108 Overall, our approach ties together among-clade variation in rates, ages, richness, and
109 traits using phylogenetic path analyses, to our knowledge for the first time in any taxon. By
110 jointly assessing the causal contributions of ecological factors to the inferred tempo of
111 mammalian lineage diversification, we are able to elucidate their relative importance to
112 generating uneven species richness patterns. We uncover that vagility and diurnality are greater
113 causes of recent speciation-rate variation than latitude, with rate variation in turn contributing
114 more to uneven species richness than differences in clade age.
115
116 **RESULTS AND DISCUSSION**
117 **Tree-wide lineage diversification relative to the K-Pg event.** The Mammalia tree
118 shows substantial unevenness in species richness across major named clades (Fig 1a). We first
119 evaluated evidence for whether early placentals diverged before, after, or during the K-Pg event,
120 known as the short fuse, long fuse, and explosive models, respectively (*51*). The first four
121 placental divergences unambiguously preceded the K-Pg (Fig. 2a; filled circles), followed by the
122 next 21 divergences with CIs that overlap it (Fig. 2a–b). Therefore, we detect a Cretaceous
123 "fuse" of ~25-Ma between the radiation of crown Placentalia and nine of 18 crown orders (Fig.
124 2b), in line with some estimates (*32*, *52*), but longer than others (e.g., (*33*)).
125 Modeling branch-specific rates across the tree shows a pulse in both speciation and
126 extinction near the K-Pg (Fig. 2c) that remarkably matches concurrent fossil evidence for
127 increases in origination and extinction (Fig. 2d; synthesized from the Paleobiology Database
128 (*30*)), as well as tree-wide shifts to higher net diversification rates in the 5-Ma following the K-
129 Pg (Fig. S5-S7). Such dynamics of lineage turnover following the K-Pg are previously reported
130 in fossil eutherians (*51*, *53*), as attributed to selective extinction followed by ecological
131 opportunity for the surviving mammal lineages (*54*, *55*). Thus, this fossil-calibrated molecular
132 phylogeny (*28*) appears to reflect dynamics evident from the fossil record alone.
133 **Branch-specific rate shifts relative to time and traits.** We recover shifts in net
134 diversification rates at 24 consistent locations in the mammal tree (Fig. 1a, 2c, e; shifts are
135 present in ≥ 50% of maximum shift credibility trees using BAMM (*56*), see *Supplementary*
136 *Materials* Fig. S7, Table S1). The earliest rate shift occurs in either crown Placentalia (1.1x

137 higher than the median background rate of 0.138 species/lineage/Ma) or Boreoeutheria (1.6x,
138 node C in Fig. 1a). These shifts involve 18 different lineages, 15 of which are consistent
139 increases. The only rate decrease was in the strepsirrhine primates (lemurs, lorises, and galagos;
140 node O). Two other shifts are alternately up or down, depending on the tree sampled (nodes H, P;
141 Fig. 1a). This result compares to 27 rate-shifted clades detected on the original mammal
142 supertree using an earlier method (15 increasing and 12 decreasing (*19*)—but note caveats about
143 the identifiability of downshifts (*57*)). Overall, rate increases nearer the present are higher, with a
144 2.2x mean in the Miocene versus 1.3x in each the Oligocene and Eocene (Fig. 2c; df=2, F=7.772,
145 P=0.003). This result is consistent with the expectation for extinctions deeper in the tree to have
146 reduced our ability to quantify more ancient shifts (*56*, *58*), as well as fossil and molecular
147 evidence that younger clades tend to have faster rates of diversification (*21*).
148 Species in rate-shifted clades overall have dissimilar ecologies (Fig. 1b), yet share more
149 attributes than expected if idiosyncratic mechanisms were entirely fostering major radiations. We
150 note the conspicuous latitudinal pattern of alternating south-north-south endemism among major
151 rodent clades, which may relate to historical biogeographic incumbency (e.g., (*59*)). Strikingly,
152 the two largest rate increases (4.0x and 3.2x) occurred in lineages with disparate life modes but
153 similar propensities for genetic isolation: the fossorial tuco-tucos of South America (*Ctenomys*,
154 node Q), and the Indo-Pacific flying foxes (*Pteropus*, node J; Fig. 1a). Thus, small burrowers and
155 large flyers both show similar signatures of recent and rapid speciation under conditions of
156 insularity, although in subterranean and oceanic realms, respectively. Tree-wide tests of trait-
157 dependent speciation suggest that high vagility is marginally associated with novel rate regimes
158 (STRAPP (*60*) one-tailed test, P = 0.08), which is contrary to the inverse vagility-to-speciation
159 relationship we expected (*39*, *40*). However, these tests are complicated by the fact that many
160 high-vagility lineages are also diurnal, and diurnality is a clearly associated with shifts to higher
161 speciation-rate regimes (P = 0.027; Fig. S8). Diurnality-associated rate shifts in simian primates,
162 carnivorans, cows, and whales (shifts N, D-F, and Q; Fig. 1a) also contain a majority of high-
163 vagility species (>1 km natal dispersal distance), and many with large latitudinal breadths (Fig.
164 1b). We thus highlight the need to tease apart the relative contributions of vagility, latitude, and
165 diurnality to understand their effects upon rate heterogeneity in mammalian clades.
166 **Named clade rate variation.** Beyond rate-shifted clades, we consider diversification-rate
167 variation within the five most speciose placental orders (Fig. 2e-f). Testing fits to diversification

168 models of rate-variable processes through time (RV, exponential or linear; (*61*)) versus rate-
169 constant ones (RC, single rates of birth or death), we find greater fits to RV models in five of the
170 12 named subclades examined (Fig. 2f; Table S2). The mouse-related clade of rodents (clade 20
171 in Figs. 1, 2f) has a branching pattern best fit by RV processes in all 100 trees examined, as
172 expected from the seven branch-specific rate shifts already uncovered in that clade (nodes R-X in
173 Figs. 1, 2). Shrews, catarrhine primates, and the cow- and whale-related clades of artiodactyls
174 join mice in showing greater RV fits than expected from RC simulation, as well as one rate shift
175 each (clades 6, 15, 10, and 11; Fig. 2f).
176 Since jump-shift processes were not directly compared to time-varying RV ones, or to
177 tree-wide shift scenarios (Fig. S5-S7), these models were not differentiable by our tests. In
178 theory, they may require considerably more fossil data to be identifiable (*62*). Nevertheless,
179 clade-specific fossil and molecular evidence supports our assertion that ancestral whales and
180 dolphins entered a novel macroevolutionary regime, including selection toward larger body sizes
181 (*56*, *60*, *61*, *63*). Bats, on the other hand, display an inconsistent fit to RV models of
182 diversification (clades 12-13, Fig. 2f), and an inconsistent number of rate shifts between our
183 study (six, nodes G-L, Fig. 1a) and a previous one (two, nodes H and J; (*64*)). We suggest that
184 high levels of topological uncertainty, which is arguably greater in bats than other orders (*65*), is
185 contributing to the equivocal modeling of RC, RV, and jump-shift processes across credible tree
186 sets for bats (Table S2).
187 As an additional, more sensitive, test of within-clade rate variation, we use clade-wide
188 distributions of tip-level speciation rates as assessed using the tip DR metric (*66*) (Fig. 2f).
189 Broadly, we recognize substantial heterogeneity in tip rates across the mammal tree, sometimes
190 with a few high-tip-rate species nested together with lower-rate species (Fig. 1a), resulting in
191 long right-side tails in the tip-rate distributions (positive skew, e.g., bat and rodent clades 12 and
192 18; Fig. 1a, 2f). We propose that tip rate skew measures aspects of within-clade speciation-rate
193 variation that is otherwise uncaptured by fitting *a priori* models of the diversification process
194 (Table S3), and thus offers a distinct predictor of among-clade variation in species richness.
195 **Time-slice clade richness relative to ages and rates.** The relative importance of clade
196 ages (time) versus rates of speciation and extinction (whether stochastic or ecologically
197 deterministic) as an explanation of extant diversity levels is widely debated (*8–12*, *16*, *17*).
198 Original claims that uneven trees are random outcomes of constant-rate diversification (e.g.,

199 (*67*)) have been refuted (*10*, *13*, *18*). However, past efforts to separate these hypotheses have
200 focused on named clades (e.g., (*10*)), which are biased by subjective delineation and often vast
201 age differences (mammal families range 3.8–59.0 Ma in mean crown ages; (*28*)).
202 To avoid problems associated with subjective clade definitions, we sliced phylogenies at
203 five-million-year intervals and took the tipward clades as objective units for analysis (Fig. 3).
204 Time-sliced clades thus account for the 'pull of the present' in modern trees (*58*) by analyzing
205 successive levels of rootward covariance among clade crown age, species richness, tip rate mean
206 and skew, and mean ecological traits. If time-constant rates predominate (*11*, *12*, *17*), crown ages
207 will explain the most among-clade variation in species richness. In contrast, if rate variation is
208 strong, as we already recognized for some nodes and named clades (Fig. 2) and expect from
209 varying ecological regimes (*7*, *19*, *39*, *68*), diversification rates will have the greater explanatory
210 power.
211 We find that clade age and richness are positively correlated—yet significantly less so
212 than the unique effects of tip rate mean and skew on richness (Fig. 4, multivariate PGLS; Fig.
213 S10 for univariate and taxon-based results). Critically, clade tip rate mean has stronger effects on
214 richness than expected from simulated birth-death trees containing only stochastic rate variation
215 (Fig. 4b). Clade tip rate skew is also significant, especially so at deeper time slices (Fig. 4c),
216 confirming that single speed-ups in diversification within a clade (e.g., due to a rate shift in one
217 lineage) can drive much of its overall species richness today. These analyses are robust to the
218 influence of species that are missing DNA sequences and imputed (Fig. S10). Our findings thus
219 support arguments that 'ecology' (broadly defined to include any extrinsic or intrinsic factor that
220 alters macroevolutionary-rate processes) is a greater cause of species richness variation than time
221 (*16*); however, both clearly contribute to observed richness (adjusted-R^2: 0.88 full model versus
222 0.74 with tip rate mean only and 0.26 with crown age only, means of 100-tree PGLS among 35-
223 Ma clades). Jointly analyzing richness determinants in time-sliced clades offers an objective way
224 to assess age and rate effects that, in turn, enables tests for which ecological factors are driving
225 that rate variation.
226 **Linking uneven rate variation to ecological factors.** We performed phylogenetic path
227 analysis (*69*) to assess the hypothesized effects of species vagility (*39*, *40*), latitude (*22*, *23*), and
228 diurnality (*48*) upon the joint, yet unequal, contributions of rates and ages to extant species
229 richness variation (Fig. 5, *Methods*, Fig. S4). Here, the time-sliced clades allow us to distinguish

230 trait-rate dynamics that are localized near the species level (if traits drive ephemeral speciation
231 (*44*) or if they evolved very recently) from those that occur deeper in the tree and persist (if traits
232 evolved anciently and did not affect extinction rates). Our assembly of species-level traits across
233 Mammalia (Fig. 1b) enables us to directly pass information to clade-level means, thereby
234 summarizing the ecological 'essence' of that clade for a given trait. However, we note that other
235 statistical moments (e.g., trait variance or skew) may prove useful for future study.
236 At the species level, we find that low-vagility mammals have higher tip speciation rates,
237 especially in herbivores and carnivores (Fig. 5a; ecological trait ~ rate PGLS (*70*)). Effects of
238 vagility on clade tip rate mean are weakened at deeper time slices, where they are instead
239 recorded on tip rate skew (Fig. 5b). We interpret these short-lived effects of vagility on
240 speciation rates as consistent with expectations that nascent allopatric species are produced at a
241 high rate, but are ephemeral, going extinct before they can expand their geographic range (*39*,
242 *40*, *44*, *71*). While the nearly 20% of mammal species that are endemic to islands complicates
243 our allometric vagility index, we note that the ~10-million-year 'threshold' whereby low-vagility
244 lineages find an adaptive zone, evolve greater vagility, or vanish is robust to multiple sensitivity
245 tests (Fig. S13-S14). The influence of vagility on mammal diversification, however, might be
246 non-linear as it is in birds (e.g., humped (*39*) or sigmoidal (*43*)).
247 To test the causal role of environmental stability in the generation of mammalian tree
248 shape (*3*, *23*, *45*), we evaluate the impact of latitudinal centroid distance from the equator upon
249 speciation rates. Contrary to the expectations of ephemeral speciation processes driving recent,
250 high rates of speciation at temperate latitudes (*22*, *23*, *45*), we find no effect of absolute latitude
251 on tip-level speciation (Fig. 5a). Instead, strong positive associations with latitude only arise at
252 deeper time slices, and without any corresponding effects on clade tip rate skew (Fig. 5b).
253 Similarly weak latitude-to-rate effects in young clades and species of birds (*22*, *45*, *66*, *72*)
254 appear to emphasize that species turnover cycles are erasing a portion of the latitudinal effect.
255 We suggest that the traditionally invoked tropical 'cradle' (higher speciation) and 'museum'
256 (lower extinction (*3*)) should re-focus upon the *combined turnover* of those processes and test
257 whether extratropical species are 'cycled' faster than tropical species. Extratropical lineages may
258 not cycle fully, but instead persist through climatic oscillations in glacial refugia (*73*). In that
259 case, the Eocene-Oligocene (~34 Ma) expansion of temperate habitats (*3*) may have initiated
260 converse latitudinal gradients in species turnover rates and total richness. Within North America,

261 the fossil record suggests the latitudinal gradient in mammalian richness was not established
262 until ~15 Ma (*74*).
263 Lastly, we queried the effect of diurnality, a core behavioral trait thought of as a temporal
264 niche innovation (*48*). We find that repeated origins of daytime activity since the late Eocene
265 (~35 Ma (*48*, *49*)) are associated with faster speciation, both at the present (Fig. 5a) and among
266 time-sliced clades at 10 Ma (Fig. 5b). These findings complement the signature of greater diurnal
267 activity on rate-shifted clades (Fig. S8), as well as place previous findings of rapid diversification
268 in diurnal lineages of primates (*50*) in a broader context. We suggest that inverse effects of
269 diurnality on tip rate skew at deeper time slices (Fig. 5b) are misleading given the evolution of
270 daytime activity ~35 Ma, well after a 'nocturnal bottleneck' among K-Pg-surviving mammals
271 (*48*, *49*). We posit that greater daytime activity is an example of an adaptive divergence in niche
272 traits that has decreased extinction rates via competitive release (i.e., an 'ecological opportunity';
273 (*68*, *75*)), and therefore led to greater species richness via persistence.
274
275 **CONCLUSION**
276 Our analyses here connect ecological factors to their time-scale-dependent effects on
277 speciation and diversification in mammals. We detect cross-clade signatures of intrinsic
278 (vagility, activity pattern) and extrinsic (latitude) factors driving aspects of lineage
279 diversification at nested phylogenetic levels. We hypothesize that two main processes are at
280 work. First, turnover-associated speciation is acting on short timescales due to geographic
281 isolation among low-vagility species, and on longer time scales, from the dynamics of
282 extratropical climates. Second, persistence-associated speciation is occurring in diurnal lineages
283 as an example of a trait that adaptively couples greater speciation with lower extinction rates.
284 Traversing from the first to second macroevolutionary mode may be possible if otherwise
285 ephemeral allopatric species enter novel regions of ecological space, either via niche evolution or
286 extrinsic opportunity, to then differentially persist under lower extinction risk (*44*, *68*, *71*, *75*).
287 Future tests that leverage direct measurements of fossil extinction rates in lineages that have
288 evolved low vagility or diurnality will be valuable for assessing the frequency of these
289 contrasting diversification modes.
290 Overall, we show that ecological factors influence speciation rates, but the effects
291 manifest at different hierarchical levels of the tree due to apparent differences in associated

292 lineage turnover. The longstanding gradient of greater tropical than temperate environmental
293 stability has led to longer species durations for tropical mammals. Geologically recent processes
294 associated with species turnover or adaptive persistence are not yet studied for most of life, but
295 our results for mammals suggest that lineage-level gradients in these novelty-originating
296 processes have causes that are rooted in the dynamics of population-level gene flow. Efforts to
297 connect evolutionary levels from individual organisms to speciose clades thus appear most
298 promising for understanding the causes and consequences of geographically and
299 phylogenetically uneven species richness across the broader tree of life.
300

301 **METHODS**

302 **Mammalian phylogeny and species trait data.** We leveraged the recently constructed
303 species-level mammal trees of Upham et al. (*28*) to conduct all analyses. Briefly, these
304 phylogenies include 5,804 extant and 107 recently extinct species in credible sets of 10,000 trees.
305 They are built using a 'backbone-and-patch' framework that used two stages of Bayesian
306 inference to integrate age and topological uncertainty, and incorporate 1,813 DNA-lacking
307 species using probabilistic constraints (available at vertlife.org/phylosubsets). We compared
308 credible sets of trees built using node-dated backbones (17 fossil calibrations) and tip-dated
309 backbones (matrix of modern and Mesozoic mammals), as well as taxonomically completed
310 trees (5911 species) versus trees of DNA-only species without topology constraints (4098
311 species).

312 Our workflow for gathering trait data involved (i) unifying multiple trait taxonomies
313 (e.g., EltonTraits v1.0 (*76*), PanTHERIA (*77*)) to our phylogeny's master taxonomy; and (ii)
314 interpolating home range area and vagility to the species level using known allometric
315 relationships in mammals (Fig. S2). Vagility was calculated as the maximum natal dispersal
316 distance per individual (km) and interpolated for each species following our updated version of
317 Whitmee and Orme's (*41*) best-fit equation, which applies species means of body mass, home
318 range, and geographic range (Fig. S3). Note that our vagility index does not account for
319 locomotor abilities (e.g., flying or arboreality), but rather captures aspects of space use that scale
320 allometrically across mammals.

321 **Tip-level speciation rates.** We calculated per-species estimates of expected pure-birth
322 diversification rates for the instantaneous present moment (tips of the tree) using the inverse of

323 the equal splits measure (*66*, *78*). This metric has been called 'tip-level diversification rate' (tip
324 DR) because it measures recent diversification processes among extant species (*79*). However, to
325 avoid confusion with 'net diversification', for which tip DR is misleading when extinction is
326 very high (relative extinction >0.8 (*80*)), we here refer to tip DR as a tip-level speciation rate
327 metric. At the tip level, we show that tip DR is tightly associated with model-based estimators of
328 speciation and net diversification rates in our trees (Fig. S1a). At the clade-level, we measure
329 'clade tip speciation mean' as the harmonic mean of tip DR among species, which is known to
330 converge to the maximum likelihood estimator of pure-birth diversification rate in clades with
331 >10 species (*66*, *78*). We show that clade tip DR mean indeed best approximates pure-birth clade
332 rates for time-sliced clades in our mammal trees (R^2: ~0.7 versus ~0.5 for birth-death speciation
333 and net diversification rates; Fig. S1b).

334 **Branch-specific and tree-wide rate shifts.** We performed searches for
335 macroevolutionary shifts using BAMM v2.5 (*56*), a reversible-jump algorithm for sampling
336 birth-death rate regimes without a prior hypothesis. We evaluated the number and location of
337 rate shifts on 10 trees from the node-dated sample of complete mammal trees. We summarized
338 across the most likely shifts per tree—called maximum shift credibility (MSC) sets (Fig. S7)—
339 using the ratio of the mean net diversification rate of all branches inside the shifted clade (clade
340 rate) and outside that clade (background rate) to calculate the rate shift magnitude and direction
341 for each MSC set (Table S1). For tree-wide rate shifts, we compared results from TreePar (*34*)
342 and CoMET (*81*) (see details in Fig. S5-S6).

343 **Comparisons with fossil genus diversification.** To assess the congruence of our
344 molecular phylogeny-based rate estimates with rates estimated from the fossil record, we
345 analyzed Mammalia fossil occurrence data from the Paleobiology Database (*30*). Grouping by
346 genus after excluding ichnotaxa and uncertain genera, we recovered 71,928 occurrences of 5300
347 genera, which we then binned in 10-Ma intervals (taxa spanning boundaries go in both bins) and
348 used shareholder quorum subsampling (SQS (*82*); quorum size: 0.5) to maximize the uniformity
349 of coverage. We then calculated corresponding origination and extinction rates per stage using
350 the per-capita rate method (*83*).

351 **Likelihood testing for models of diversification.** We analyzed the branching times of
352 27 named subclades (11 orders and 16 suborders) that contained ≥ 25 species. For each subclade,
353 we tested 10 models developed by Morlon et al. (*61*): two rate-constant (RC) models, constant

354 pure-birth and birth-death; and eight rate-variable (RV) models, with exponentially and linearly
355 time-varying rates. We fit models for 100 trees of the empirical subclades and their matching
356 RC-simulated trees (null models, simulated under the empirical extinction fractions of ~ε=0.65
357 over 100 trees using the "pbtree" function in phytools (*84*)). Subtracting AICc scores of the best-
358 fitting RC and RV models provided the $\Delta AIC_{RC\text{-}RV}$ test statistic (*85*) per tree and subclade for
359 comparison to the simulated null distribution (alpha=0.05; see Table S2).

360 **Time-sliced clades and clade-level tests of species richness variation.** To objectively
361 define clades, we arbitrarily drew lines (referred to as "time slices") at 5-Ma intervals and took
362 the resulting *tipward* (all the way to the extant tip) monophyletic clades as non-nested units of
363 analysis. The *rootward* relationships of those clades (the "rootward backbone") was retained for
364 each interval, giving the expected covariance structure among clades when performing
365 phylogenetic generalized least squares (PGLS) analyses (see Fig. 3 for illustration). We used the
366 "treeSlice" function in phytools to construct clade sets across Mammalia trees and the three sets
367 of RC simulations, empirical (ε=0.65), low (ε=0.2), and high (ε=0.8), also comparing our results
368 to analyses on traditional taxon-based clades (genera, families, and orders; Fig. S10-S12). All
369 PGLS was performed excluding extinct species, using Pagel's "lambda" transformation in
370 phylolm (optimized for large trees (*86*)), and repeating the analysis across 100 or 1000 trees. We
371 also performed multivariate analyses including percent of DNA-sampled species per clade to test
372 whether our results are unaffected by imputing DNA-missing species (Fig. S10).

373 **Tip-level tests of speciation-rate correlates.** To examine correlative structures
374 underlying observed tip-rate variation, we performed tip-level PGLS analyses between species'
375 ecological traits and tip DR values across 1000 trees, focusing on a 5675-species data set that
376 excluded all extinct (n=107) and marine (n=129) species. We followed Freckleton et al. (*70*) in
377 using trait ~ rate models in our tip-level PGLS analyses to avoid identical residuals in the
378 dependent variable (i.e., sister species have identical tip DR values, which otherwise violates the
379 assumed within-variable data independence in bivariate normal distributions). The trait ~ rate
380 approach was previously applied using tip DR in univariate contexts (*87*) (see Fig. S13-S14 for
381 sensitivity tests).

382 **Clade-level tests of speciation-rate correlates.** At the clade level, univariate PGLS was
383 performed typically (rate ~ trait models), since clade tip DR mean gave independent values to
384 sister clades. These analyses were conducted on 1000 trees by analogy with those previous,

except that per-clade trait summaries were standardized predictors (mean centered, standard deviation scaled) using geometric means for vagility and arithmetic means otherwise. We also performed tests for trait-dependent speciation using rate-shifted clades identified in BAMM runs on 10 mammal trees (STRAPP (*60*) method), which corrects for phylogenetic pseudoreplication similar to PGLS except instead via the covariance structure among rate regimes (see Fig. S8).

Phylogenetic path analyses. We performed path analysis aiming to fully resolve correlational structures and thereby translate from the language of statistical association to causality. For phylogenetic path analyses, we used PGLS to test statements of conditional independence (*69*) across 27 pre-selected path models (Fig. S4). For each tree and clade set, we used "phylopath" (*88*) to analyze models and perform conditional model averaging. Time-sliced clades at 10-, 30-, and 50-Ma intervals were analyzed and compared to analogous results using taxon-based clades (Fig. S12).

Acknowledgments: We thank I. Quintero, M. Landis, D. Schluter, A. Mooers, A. Pyron, G. Thomas, D. Greenberg, S. Upham and E. Florsheim for conceptual discussions that improved this study; B. Patterson, K. Rowe, J. Brown, T. Colston, T. Peterson, D. Field, T. Stewart, J. Davies, and three anonymous reviewers for comments on earlier drafts; and M. Koo, A. Ranipeta, and J. Hart for database help. Artwork from phylopic.org and open source fonts. **Funding:** The NSF VertLife Terrestrial grant to W.J. and J.E. (DEB 1441737 and 1441634) and NSF grant DBI-1262600 to W.J. supported this work. **Author contributions:** NSU and WJ conceived the study; NSU and JAE collected and curated the data; NSU performed all analyses and wrote the first draft of the manuscript, with contributions to revisions from all co-authors. **Competing interests:** None. **Data and material availability:** All data and code is available in the manuscript and after publication on Dryad (also to be available at github.com/n8upham/).

References

1. P. V. A. Fine, R. H. Ree, Evidence for a Time-Integrated Species-Area Effect on the Latitudinal Gradient in Tree Diversity. *Am. Nat.* **168**, 796–804 (2006).
2. D. Jablonski, K. Roy, J. W. Valentine, Out of the Tropics: Evolutionary dynamics of the latitudinal diversity gradient. *Science*. **314**, 102–106 (2006).
3. G. G. Mittelbach, D. W. Schemske, H. V. Cornell, A. P. Allen, J. M. Brown, M. B. Bush, S. P. Harrison, A. H. Hurlbert, N. Knowlton, H. A. Lessios, C. M. McCain, A. R. McCune, L. A. McDade, M. A. McPeek, T. J. Near, T. D. Price, R. E. Ricklefs, K. Roy, D. F. Sax, D. Schluter, J. M. Sobel, M. Turelli, Evolution and the latitudinal diversity gradient: speciation, extinction and biogeography. *Ecol. Lett.* **10**, 315–331 (2007).
4. W. Jetz, P. V. A. Fine, Global Gradients in Vertebrate Diversity Predicted by Historical Area-Productivity Dynamics and Contemporary Environment. *PLOS Biol.* **10**, e1001292 (2012).
5. R. Jansson, G. Rodríguez-Castañeda, L. E. Harding, What Can Multiple Phylogenies Say About the Latitudinal Diversity Gradient? A New Look at the Tropical Conservatism, Out of the Tropics, and Diversification Rate Hypotheses. *Evolution*. **67**, 1741–1755 (2013).
6. J. C. Willis, *Age and Area* (Cambridge University Press, Cambridge, 1922).
7. A. O. Mooers, S. B. Heard, Inferring Evolutionary Process from Phylogenetic Tree Shape. *Q. Rev. Biol.* **72**, 31–54 (1997).
8. M. A. McPeek, J. M. Brown, Clade age and not diversification rate explains species richness among animal taxa. *Am. Nat.* **169** (2007).
9. J. J. Wiens, The causes of species richness patterns across space, time, and clades and the role of "ecological limits". *Q. Rev. Biol.* **86**, 75–96 (2011).
10. D. L. Rabosky, G. J. Slater, M. E. Alfaro, Clade age and species richness are decoupled across the eukaryotic tree of life. *PLoS Biol.* **10**, e1001381 (2012).
11. S. B. Hedges, J. Marin, M. Suleski, M. Paymer, S. Kumar, Tree of life reveals clock-like speciation and diversification. *Mol. Biol. Evol.*, msv037 (2015).
12. R. E. Ricklefs, Global diversification rates of passerine birds. *Proc. R. Soc. Lond. B-Biol. Sci.* **270**, 2285–2291 (2003).
13. M. G. B. Blum, O. François, Which Random Processes Describe the Tree of Life? A Large-Scale Study of Phylogenetic Tree Imbalance. *Syst. Biol.* **55**, 685–691 (2006).
14. A. B. Phillimore, T. D. Price, Density-dependent cladogenesis in birds. *PLoS Biol.* **6**, e71 (2008).
15. D. L. Rabosky, Ecological limits and diversification rate: alternative paradigms to explain the variation in species richness among clades and regions. *Ecol. Lett.* **12**, 735–743 (2009).
16. T. D. Price, The roles of time and ecology in the continental radiation of the Old World leaf warblers (*Phylloscopus* and *Seicercus*). *Philos. Trans. R. Soc. Lond. B Biol. Sci.* **365**, 1749–1762 (2010).
17. C. Venditti, A. Meade, M. Pagel, Phylogenies reveal new interpretation of speciation and the Red Queen. *Nature*. **463**, 349–352 (2010).
18. T. J. Davies, A. P. Allen, L. Borda-de-Água, J. Regetz, C. J. Melián, Neutral Biodiversity Theory Can Explain the Imbalance of Phylogenetic Trees but Not the Tempo of Their Diversification. *Evolution*. **65**, 1841–1850 (2011).
19. A. Purvis, S. A. Fritz, J. Rodríguez, P. H. Harvey, R. Grenyer, The shape of mammalian phylogeny: patterns, processes and scales. *Philos. Trans. R. Soc. Lond. B Biol. Sci.* **366**, 2462–2477 (2011).

20. D. S. Moen, H. Morlon, Why does diversification slow down? *Trends Ecol. Evol.* **29**, 190–197 (2014).
21. L. F. H. Diaz, L. J. Harmon, M. T. C. Sugawara, E. T. Miller, M. W. Pennell, Macroevolutionary diversification rates show time dependency. *Proc. Natl. Acad. Sci.*, 201818058 (2019).
22. J. T. Weir, D. Schluter, The Latitudinal Gradient in Recent Speciation and Extinction Rates of Birds and Mammals. *Science*. **315**, 1574–1576 (2007).
23. A. D. Cutter, J. C. Gray, Ephemeral ecological speciation and the latitudinal biodiversity gradient. *Evolution*. **70**, 2171–2185 (2016).
24. D. Jablonski, Species Selection: Theory and Data. *Annu. Rev. Ecol. Evol. Syst.* **39**, 501–524 (2008).
25. J. Alroy, Small mammals have big tails in the tropics. *Glob. Ecol. Biogeogr.* **0** (2019), doi:10.1111/geb.12912.
26. J. M. Beaulieu, B. C. O'Meara, Can we build it? Yes we can, but should we use it? Assessing the quality and value of a very large phylogeny of campanulid angiosperms. *Am. J. Bot.* **105**, 417–432 (2018).
27. C. J. Burgin, J. P. Colella, P. L. Kahn, N. S. Upham, How many species of mammals are there? *J. Mammal.* **99**, 1–14 (2018).
28. N. S. Upham, J. A. Esselstyn, W. Jetz, Inferring the mammal tree: species-level sets of phylogenies for questions in ecology, evolution, and conservation. *PLOS Biol.* (2019).
29. T. W. Davies, M. A. Bell, A. Goswami, T. J. D. Halliday, Completeness of the eutherian mammal fossil record and implications for reconstructing mammal evolution through the Cretaceous/Paleogene mass extinction. *Paleobiology* (2017), , doi:10.1017/pab.2017.20.
30. J. Alroy, M. D. Uhen, P. D. Mannion, C. Jaramillo, M. T. Carrano, L. W. van den Hoek Ostende, Taxonomic occurrences of Mammalia recorded in Fossilworks, the Evolution of Terrestrial Ecosystems database, and the Paleobiology Database. Fossilworks. http://fossilworks.org. (2018).
31. C. V. Bennett, P. Upchurch, F. J. Goin, A. Goswami, Deep time diversity of metatherian mammals: implications for evolutionary history and fossil-record quality. *Paleobiology*. **44**, 171–198 (2018).
32. R. W. Meredith, J. E. Janečka, J. Gatesy, O. A. Ryder, C. A. Fisher, E. C. Teeling, A. Goodbla, E. Eizirik, T. L. L. Simão, T. Stadler, D. L. Rabosky, R. L. Honeycutt, J. J. Flynn, C. M. Ingram, C. Steiner, T. L. Williams, T. J. Robinson, A. Burk-Herrick, M. Westerman, N. A. Ayoub, M. S. Springer, W. J. Murphy, Impacts of the Cretaceous Terrestrial Revolution and KPg Extinction on Mammal Diversification. *Science*. **334**, 521–524 (2011).
33. O. R. P. Bininda-Emonds, M. Cardillo, K. E. Jones, R. D. E. MacPhee, R. M. D. Beck, R. Grenyer, S. A. Price, R. A. Vos, J. L. Gittleman, A. Purvis, The delayed rise of present-day mammals. *Nature*. **446**, 507–512 (2007).
34. T. Stadler, Mammalian phylogeny reveals recent diversification rate shifts. *Proc. Natl. Acad. Sci.* **108**, 6187–6192 (2011).
35. S. A. Price, S. B. Hopkins, K. K. Smith, V. L. Roth, Tempo of trophic evolution and its impact on mammalian diversification. *Proc. Natl. Acad. Sci. USA*. **109**, 7008–7012 (2012).
36. J. Rolland, F. L. Condamine, F. Jiguet, H. Morlon, Faster Speciation and Reduced Extinction in the Tropics Contribute to the Mammalian Latitudinal Diversity Gradient. *PLOS Biol.* **12**, e1001775 (2014).

37. T. S. Kuhn, A. Ø. Mooers, G. H. Thomas, A simple polytomy resolver for dated phylogenies. *Methods Ecol. Evol.* **2**, 427–436 (2011).
38. S. Faurby, J.-C. Svenning, A species-level phylogeny of all extant and late Quaternary extinct mammals using a novel heuristic-hierarchical Bayesian approach. *Mol. Phylogenet. Evol.* **84**, 14–26 (2015).
39. E. Mayr, *Animal species and evolution* (Belknap, Cambridge, MA, 1963).
40. Y. Kisel, T. G. Barraclough, Speciation Has a Spatial Scale That Depends on Levels of Gene Flow. *Am. Nat.* **175**, 316–334 (2010).
41. S. Whitmee, C. D. L. Orme, Predicting dispersal distance in mammals: a trait-based approach. *J. Anim. Ecol.* **82**, 211–221 (2013).
42. Belliure, Sorci, Møller, Clobert, Dispersal distances predict subspecies richness in birds. *J. Evol. Biol.* **13**, 480–487 (2000).
43. S. Claramunt, E. P. Derryberry, J. V. Remsen, R. T. Brumfield, High dispersal ability inhibits speciation in a continental radiation of passerine birds. *Proc. R. Soc. Lond. B Biol. Sci.* **279**, 1567–1574 (2012).
44. E. B. Rosenblum, B. A. J. Sarver, J. W. Brown, S. D. Roches, K. M. Hardwick, T. D. Hether, J. M. Eastman, M. W. Pennell, L. J. Harmon, Goldilocks Meets Santa Rosalia: An Ephemeral Speciation Model Explains Patterns of Diversification Across Time Scales. *Evol. Biol.* **39**, 255–261 (2012).
45. D. Schluter, M. W. Pennell, Speciation gradients and the distribution of biodiversity. *Nature*. **546**, 48–55 (2017).
46. Soria-Carrasco Víctor, Castresana Jose, Diversification rates and the latitudinal gradient of diversity in mammals. *Proc. R. Soc. B Biol. Sci.* **279**, 4148–4155 (2012).
47. C. A. Botero, R. Dor, C. M. McCain, R. J. Safran, Environmental harshness is positively correlated with intraspecific divergence in mammals and birds. *Mol. Ecol.* **23**, 259–268 (2014).
48. M. P. Gerkema, W. I. L. Davies, R. G. Foster, M. Menaker, R. A. Hut, The nocturnal bottleneck and the evolution of activity patterns in mammals. *Proc R Soc B*. **280**, 20130508 (2013).
49. R. Maor, T. Dayan, H. Ferguson-Gow, K. E. Jones, Temporal niche expansion in mammals from a nocturnal ancestor after dinosaur extinction. *Nat. Ecol. Evol.* **1**, 1889 (2017).
50. J. H. Arbour, S. E. Santana, A major shift in diversification rate helps explain macroevolutionary patterns in primate species diversity. *Evolution*. **71**, 1600–1613 (2017).
51. J. D. Archibald, D. H. Deutschman, Quantitative Analysis of the Timing of the Origin and Diversification of Extant Placental Orders. *J. Mamm. Evol.* **8**, 107–124 (2001).
52. M. dos Reis, J. Inoue, M. Hasegawa, R. J. Asher, P. C. J. Donoghue, Z. Yang, Phylogenomic datasets provide both precision and accuracy in estimating the timescale of placental mammal phylogeny. *Proc. R. Soc. Lond. B Biol. Sci.* **279**, 3491–3500 (2012).
53. M. M. Pires, B. D. Rankin, D. Silvestro, T. B. Quental, Diversification dynamics of mammalian clades during the K–Pg mass extinction. *Biol. Lett.* **14**, 20180458 (2018).
54. D. M. Grossnickle, E. Newham, Therian mammals experience an ecomorphological radiation during the Late Cretaceous and selective extinction at the K–Pg boundary. *Proc R Soc B*. **283**, 20160256 (2016).
55. D. M. Grossnickle, S. M. Smith, G. P. Wilson, Untangling the Multiple Ecological Radiations of Early Mammals. *Trends Ecol. Evol.* (2019), doi:10.1016/j.tree.2019.05.008.

56. D. L. Rabosky, Automatic detection of key innovations, rate shifts, and diversity-dependence on phylogenetic trees. *PLoS ONE*. **9**, e89543 (2014).
57. B. R. Moore, K. M. A. Chan, M. J. Donoghue, in *Phylogenetic Supertrees*, O. R. P. Bininda-Emonds, Ed. (Springer Netherlands, 2004; http://link.springer.com/chapter/10.1007/978-1-4020-2330-9_23), *Computational Biology*, pp. 487–533.
58. S. Nee, E. C. Holmes, R. M. May, P. H. Harvey, Extinction rates can be estimated from molecular phylogenies. *Philos. Trans. R. Soc. Lond. B-Biol. Sci.* **344**, 77–82 (1994).
59. J. J. Schenk, K. C. Rowe, S. J. Steppan, Ecological opportunity and incumbency in the diversification of repeated continental colonizations by muroid rodents. *Syst. Biol.* **62**, 837–864 (2013).
60. D. L. Rabosky, H. Huang, A Robust Semi-Parametric Test for Detecting Trait-Dependent Diversification. *Syst. Biol.* **65**, 181–193 (2016).
61. H. Morlon, T. L. Parsons, J. B. Plotkin, Reconciling molecular phylogenies with the fossil record. *Proc. Natl. Acad. Sci.* **108**, 16327–16332 (2011).
62. S. Louca, M. W. Pennell, Phylogenies of extant species are consistent with an infinite array of diversification histories. *bioRxiv*, 719435 (2019).
63. N. D. Pyenson, The Ecological Rise of Whales Chronicled by the Fossil Record. *Curr. Biol.* **27**, R558–R564 (2017).
64. J. J. Shi, D. L. Rabosky, Speciation dynamics during the global radiation of extant bats. *Evolution*. **69**, 1528–1545 (2015).
65. L. I. Amador, R. L. M. Arévalo, F. C. Almeida, S. A. Catalano, N. P. Giannini, Bat Systematics in the Light of Unconstrained Analyses of a Comprehensive Molecular Supermatrix. *J. Mamm. Evol.* **25**, 37–70 (2018).
66. W. Jetz, G. H. Thomas, J. B. Joy, K. Hartmann, A. O. Mooers, The global diversity of birds in space and time. *Nature*. **491**, 444–448 (2012).
67. S. Wright, The "Age and Area" Concept Extended. *Ecology*. **22**, 345–347 (1941).
68. G. G. Simpson, *The major features of evolution* (Columbia Univ Press, New York, 1953).
69. A. von Hardenberg, A. Gonzalez-Voyer, Disentangling Evolutionary Cause-Effect Relationships with Phylogenetic Confirmatory Path Analysis. *Evolution*. **67**, 378–387 (2013).
70. R. P. Freckleton, A. B. Phillimore, M. Pagel, Relating Traits to Diversification: A Simple Test. *Am. Nat.* **172**, 102–115 (2008).
71. D. Jablonski, Heritability at the Species Level: Analysis of Geographic Ranges of Cretaceous Mollusks. *Science*. **238**, 360–363 (1987).
72. D. L. Rabosky, P. O. Title, H. Huang, Minimal effects of latitude on present-day speciation rates in New World birds. *Proc R Soc B*. **282**, 20142889 (2015).
73. G. Hewitt, The genetic legacy of the Quaternary ice ages. *Nature*. **405**, 907–913 (2000).
74. J. D. Marcot, D. L. Fox, S. R. Niebuhr, Late Cenozoic onset of the latitudinal diversity gradient of North American mammals. *Proc. Natl. Acad. Sci.* **113**, 7189–7194 (2016).
75. J. B. Yoder, E. Clancey, S. Des Roches, J. M. Eastman, L. Gentry, W. Godsoe, T. J. Hagey, D. Jochimsen, B. P. Oswald, J. Robertson, B. A. J. Sarver, J. J. Schenk, S. F. Spear, L. J. Harmon, Ecological opportunity and the origin of adaptive radiations. *J. Evol. Biol.* **23**, 1581–1596 (2010).
76. H. Wilman, J. Belmaker, J. Simpson, C. de la Rosa, M. M. Rivadeneira, W. Jetz, EltonTraits 1.0: Species-level foraging attributes of the world's birds and mammals. *Ecology*. **95**, 2027–2027 (2014).

77. K. E. Jones, J. Bielby, M. Cardillo, S. A. Fritz, J. O'Dell, C. D. L. Orme, K. Safi, W. Sechrest, E. H. Boakes, C. Carbone, C. Connolly, M. J. Cutts, J. K. Foster, R. Grenyer, M. Habib, C. A. Plaster, S. A. Price, E. A. Rigby, J. Rist, A. Teacher, O. R. P. Bininda-Emonds, J. L. Gittleman, G. M. Mace, A. Purvis, PanTHERIA: a species-level database of life history, ecology, and geography of extant and recently extinct mammals. *Ecology*. **90**, 2648–2648 (2009).
78. M. Steel, A. Mooers, The expected length of pendant and interior edges of a Yule tree. *Appl. Math. Lett.* **23**, 1315–1319 (2010).
79. I. Quintero, W. Jetz, Global elevational diversity and diversification of birds. *Nature* (2018).
80. P. O. Title, D. L. Rabosky, Tip rates, phylogenies and diversification: What are we estimating, and how good are the estimates? *Methods Ecol. Evol.* **10**, 821–834 (2019).
81. M. R. May, S. Höhna, B. R. Moore, A Bayesian approach for detecting the impact of mass-extinction events on molecular phylogenies when rates of lineage diversification may vary. *Methods Ecol. Evol.* **7**, 947–959 (2016).
82. J. Alroy, Accurate and precise estimates of origination and extinction rates. *Paleobiology*. **40**, 374–397 (2014).
83. M. Foote, Origination and extinction components of taxonomic diversity: general problems. *Paleobiology*. **26**, 74–102 (2000).
84. L. J. Revell, phytools: an R package for phylogenetic comparative biology (and other things). *Methods Ecol. Evol.* **3**, 217–223 (2012).
85. D. L. Rabosky, Likelihood methods for detecting temporal shifts in diversification rates. *Evolution*. **60**, 1152–1164 (2006).
86. L. S. T. Ho, C. Ané, A Linear-Time Algorithm for Gaussian and Non-Gaussian Trait Evolution Models. *Syst. Biol.* **63**, 397–408 (2014).
87. M. G. Harvey, G. F. Seeholzer, B. T. Smith, D. L. Rabosky, A. M. Cuervo, R. T. Brumfield, Positive association between population genetic differentiation and speciation rates in New World birds. *Proc. Natl. Acad. Sci.* **114**, 6328–6333 (2017).
88. W. van der Bijl, phylopath: Easy phylogenetic path analysis in R. *PeerJ*. **6**, e4718 (2018).

620 **Figure legends**

621 **Fig. 1. Species-level relationships, rates, and traits for 5,911 species of mammals globally.**
622 (**a**) The maximum clade credibility topology of 10,000 node-dated trees, with numbered clade
623 labels corresponding to orders and subclades listed in the plot periphery: Eulipoty., Eulipotyphla;
624 Carn., Carnivora; Artio., Artiodactyla. Scale in millions of years, Ma. Branches are colored with
625 tip-level speciation rates (tip DR metric) and marked with 24 inferred shifts in branch-specific
626 net diversification rates (nodes A-X; shifts with multiple circles occurred on either branch, not
627 both). Tip-level rates are reconstructed to interior branches using Brownian motion. (**b**) Per-
628 species ecological traits: allometric index of vagility (dispersal ability), diurnality (predominant
629 daytime activity), and north-south latitudinal extent (see *Methods* for details). Silhouettes are
630 from phylopic.org and open source fonts.

631 **Fig. 2. Diversification rate variation among mammal clades.** Lineage-through-time plots and
632 estimated crown ages for (**a**) all superordinal divergences (y-axis does not apply to error bars),
633 and (**b**) placental orders with crown age estimates overlapping the Cretaceous-Paleogene
634 extinction event (K-Pg, dashed gray line; means and 95% CIs; filled circle if statistically
635 different). (**c**) Rate-through-time plots for speciation, extinction, and net diversification
636 (summarized from Fig. 1 rate shifts; medians from 10 trees, 95% CIs in light gray). (**d**) Fossil
637 genus diversity through time for all Mammalia, including subsampled genus richness (quorum
638 0.5) and per-capita rates of genus origination and extinction. (**e**) Extant rates and lineage-specific
639 rate shifts for the five most speciose mammal orders (same symbols as in **c**). (**f**) Rate variation
640 within subclades of these five orders as numbered from Fig. 1; left: difference in AIC between
641 best-fit models of diversification for trees simulated under rate-constant birth-death (gray) versus
642 observed mammal trees (color; filled circle and * if ΔAIC on 100 trees is statistically different);
643 and, right: tip-level speciation rate (tip DR metric) distributions of the same simulated and
644 observed subclades (gray versus color, one tree), comparing variation in clade tip rate mean and
645 skew across 100 trees. The last 2 Ma are removed from parts **c-e** to focus on pre-recent rate
646 dynamics.

647 **Fig. 3. Explanation of time-sliced clade delimitation and summarization for testing**
648 **hypotheses.** (**a and b**) An example subclade of 64 species, the rodent family Heteromyidae, is
649 divided into time-sliced clades in the same way as for all Mammalia. Branch colors in the

650 family-level phylogeny correspond to tip-level diversification rates (tip DR) calculated on the
651 full tree, and red symbols are sized according to estimates of species vagility. An example time
652 slice for 5-Ma tipward clades is shown with summaries of tip DR mean and vagility (harmonic
653 and geometric means) to compare to clade crown age and richness. (**c**) Example Mammalia-wide
654 time slice at 35 Ma delimiting clades for multivariate PGLS (phylogenetic generalized least
655 squares) analysis on log clade richness, as was performed on 100 trees throughout this study.
656 Observed mammal clades are compared to clades from simulated rate-constant trees of the same
657 age and richness. (**d**) Results for clades defined at time-slices every 5 Ma for log clade richness
658 and its variance, as compared among empirical mammal trees and simulated trees.

659 **Fig. 4. Age and rate components of species richness variation across time-slice defined**
660 **clades. (a)** The log species richness of clades tipward of each 5-Ma time slice (dotted lines from
661 5-70 Ma) across a sample of 100 phylogenies (maximum clade credibility tree shown) is best
662 predicted jointly by clade crown age, (**b**) clade tip DR mean, and (**c**) clade tip DR skew.
663 Multivariate phylogenetic analyses of clade richness in observed trees (grey) is compared to trees
664 simulated under rate-constant birth and death with different extinction fractions, ε (colours in
665 legend; PGLS on standardized data with 95% confidence intervals [CIs] on parameter estimates).
666 Solid black lines are the observed best-fitting models given random effects of time slice and tree.

667 **Fig. 5. Connecting clade ages, rates, richness, and traits in the mammal tree of life.** (**a**, top
668 panel) Distribution of tip-level speciation rates (tip DR metric, harmonic mean of 10,000 trees)
669 relative to per-species estimates of vagility (maximum natal dispersal distance), diurnality
670 (0=nocturnal or cathemeral, 1=diurnal), and absolute value of latitude (centroid of expert maps)
671 across 5,675 species (excluding extinct and marine species). Loess smoothing lines visualize
672 general trends (blue, span=0.33). Tip-level effects (bottom panel) from univariate PGLS between
673 tip speciation rates and ecological traits subset across trophic levels (1000 trees, 95% CI, colored
674 if significant). (**b**) Phylogenetic path analysis (*69*) of putative causal relationships between traits
675 and rates leading to clade species richness for time-sliced clades. Path thickness, color, and
676 directionality denote median coefficients of model-averaged analyses. The bottom panels provide
677 per-estimate uncertainty across time slices (slope ± SE, 1000 trees). Non-zero estimates, either
678 positive (blue shades) or negative (red shades), are totaled in the right margin; paths present in
679 >500 trees are bolded and displayed in path model whereas others are dashed.

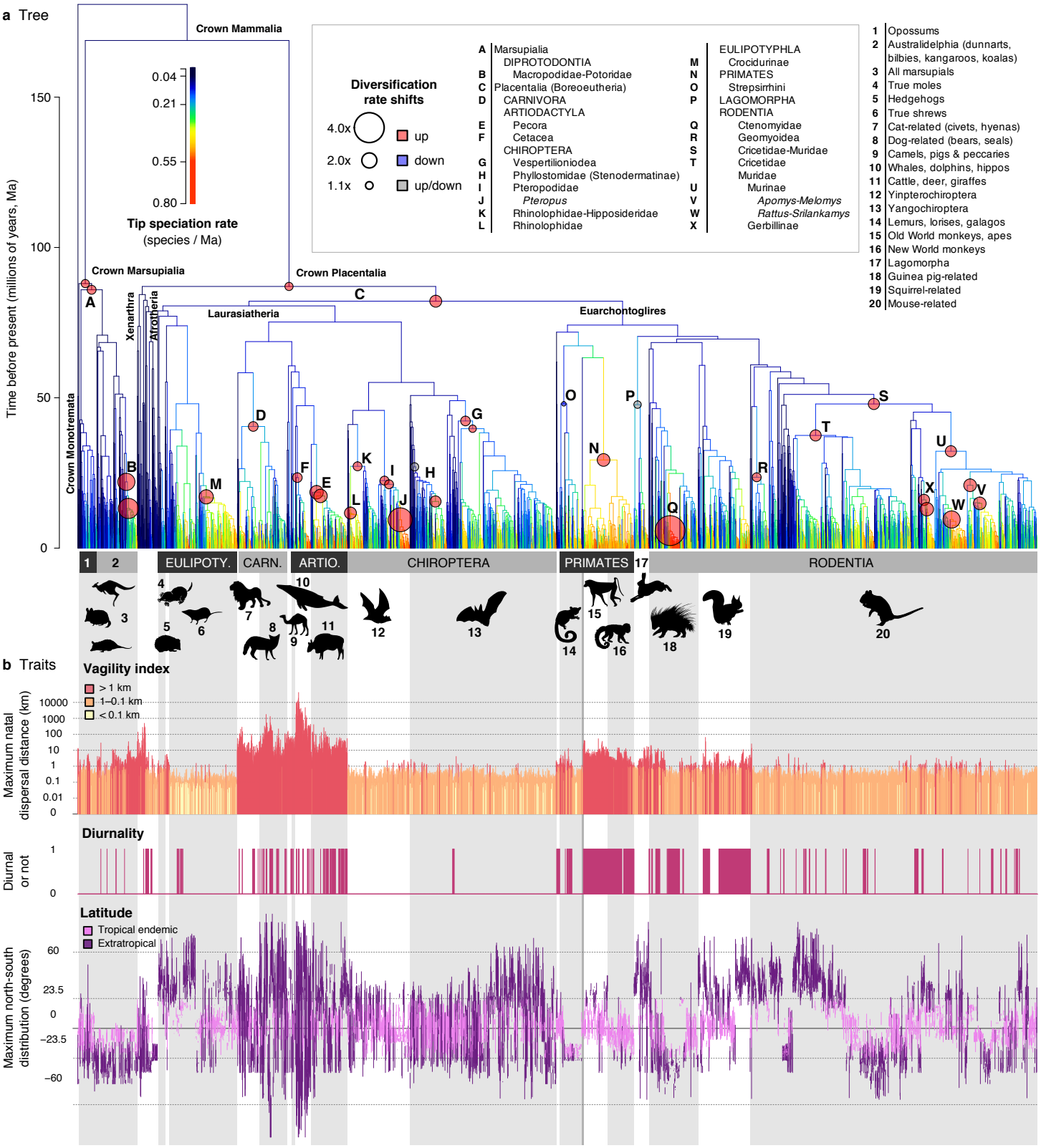

Fig. 1. Species-level relationships, rates, and traits for 5,911 species of mammals globally. (a) The maximum clade credibility topology of 10,000 node-dated trees, with numbered clade labels corresponding to orders and subclades listed in the plot periphery: Eulipoty., Eulipotyphla; Carn., Carnivora; Artio., Artiodactyla. Scale in millions of years, Ma. Branches are colored with tip-level speciation rates (tip DR metric) and marked with 24 inferred shifts in branch-specific net diversification rates (nodes A-X; shifts with multiple circles occurred on either branch, not both). Tip-level rates are reconstructed to interior branches using Brownian motion. (**b**) Per-species ecological traits: allometric index of vagility (dispersal ability), diurnality (predominant daytime activity), and north-south latitudinal extent (see *Methods* for details). Silhouettes are from phylopic.org and open source fonts.

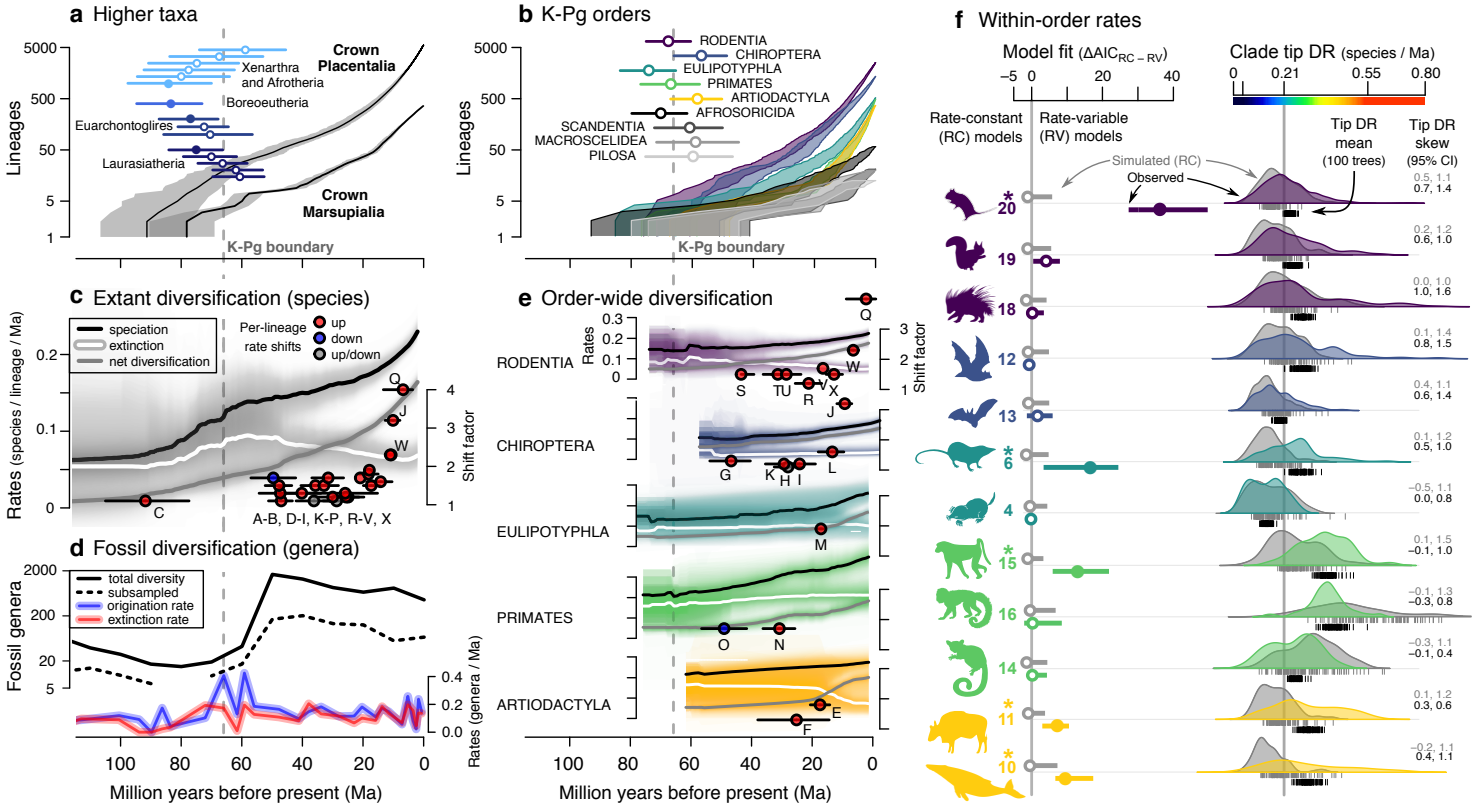

Fig. 2. Diversification rate variation among mammal clades. Lineage-through-time plots and estimated crown ages for (**a**) all superordinal divergences (y-axis does not apply to error bars), and (**b**) placental orders with crown age estimates overlapping the Cretaceous-Paleogene extinction event (K-Pg, dashed grey line; means and 95% CIs; filled circle if statistically different). (**c**) Extant rates of speciation, extinction, and net diversification through time on the full Mammalia phylogeny relative to lineage-specific shifts in net diversification (median rates from 10 trees, 95% CIs in light grey). (**d**) Fossil genus diversity through time for all Mammalia, including subsampled genus richness (quorum 0.5) and per-capita rates of genus origination and extinction. (**e**) Extant rates and lineage-specific rate shifts for the five most speciose mammal orders (same symbols as in **c**). (**f**) Rate variation within subclades of these five orders (numbers correspond to Fig. 1); left: quantified as difference in AIC between best-fit models of diversification ($\Delta AIC_{RC\text{-}RV}$ median and 95% CIs on 100 trees) for trees simulated under rate-constant birth-death (RC, grey) versus observed mammal trees (colour; * and filled circle if statistically different); and, right: example tip DR distributions of the same simulated and observed subclades (grey versus colour, one tree), comparing variation in tip DR mean and skew relative to the median for all Mammalia (grey line, 100 trees). The last 2 Ma are removed from parts **c-e** to focus on pre-recent rate dynamics.

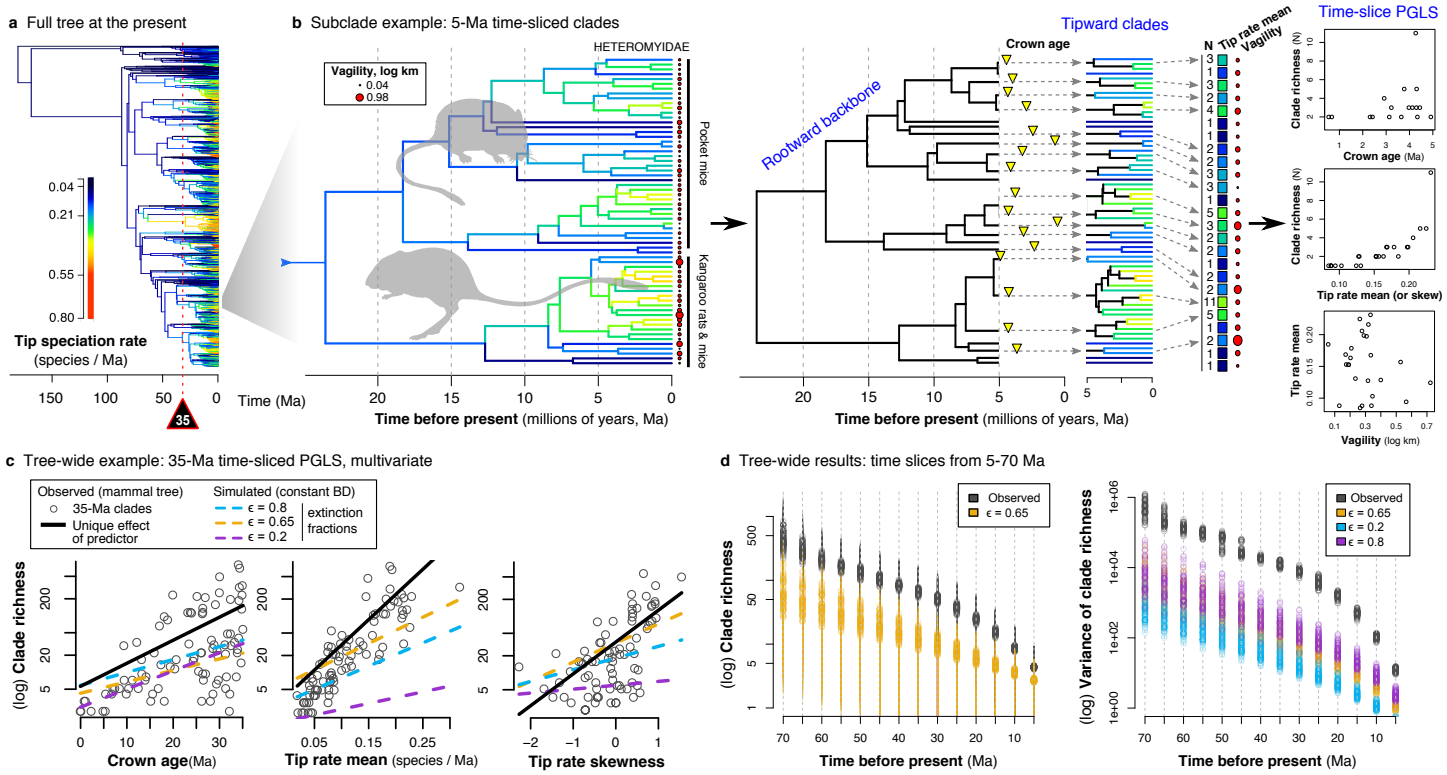

Fig. 3. Explanation of time-sliced clade delimitation and summarization for testing hypotheses. (**a and b**) An example subclade of 64 species, the rodent family Heteromyidae, is divided into time-sliced clades in the same way as for all Mammalia. Branch colors in the family-level phylogeny correspond to tip-level diversification rates (tip DR) calculated on the full tree, and red symbols are sized according to estimates of species vagility. An example time slice for 5-Ma tipward clades is shown with summaries of tip DR mean and vagility (harmonic and geometric means) to compare to clade crown age and richness. (**c**) Example Mammalia-wide time slice at 35 Ma delimiting clades for multivariate PGLS (phylogenetic generalized least squares) analysis on log clade richness, as was performed on 100 trees throughout this study. Observed mammal clades are compared to clades from simulated rate-constant trees of the same age and richness. (**d**) Results for log clade richness and its variance comparing clades defined at time-slices every 5 Ma for observed mammal trees (grey) and trees simulated with different extinction fractions (ε, colored).

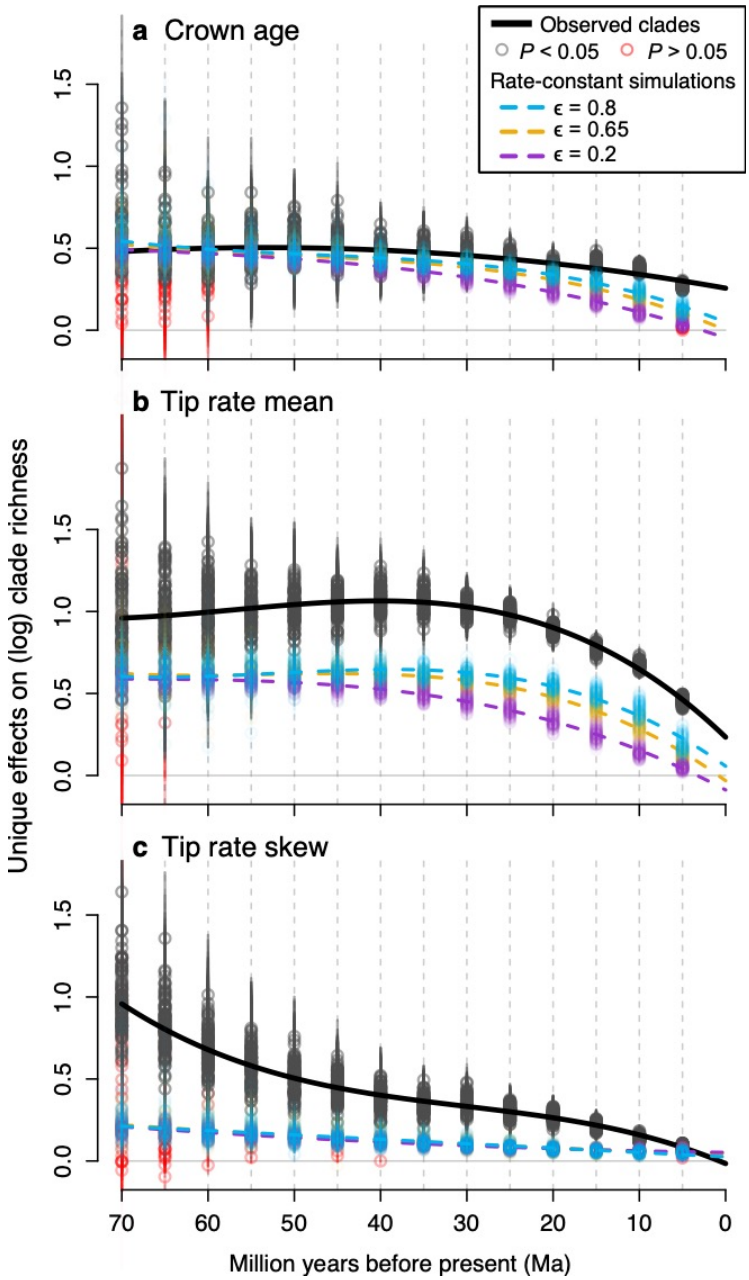

Fig. 4. Age and rate components of species richness variation across time-slice defined clades. (a) The log species richness of clades tipward of each 5-Ma time slice (dotted lines from 5-70 Ma) across a sample of 100 phylogenies (maximum clade credibility tree shown) is best predicted jointly by clade crown age, (**b**) clade tip DR mean, and (**c**) clade tip DR skew. Multivariate phylogenetic analyses of clade richness in observed trees (grey) is compared to trees simulated under rate-constant birth and death with different extinction fractions, ε (colours in legend; PGLS on standardized data with 95% confidence intervals [CIs] on parameter estimates). Solid black lines are the observed best-fitting models given random effects of time slice and tree.

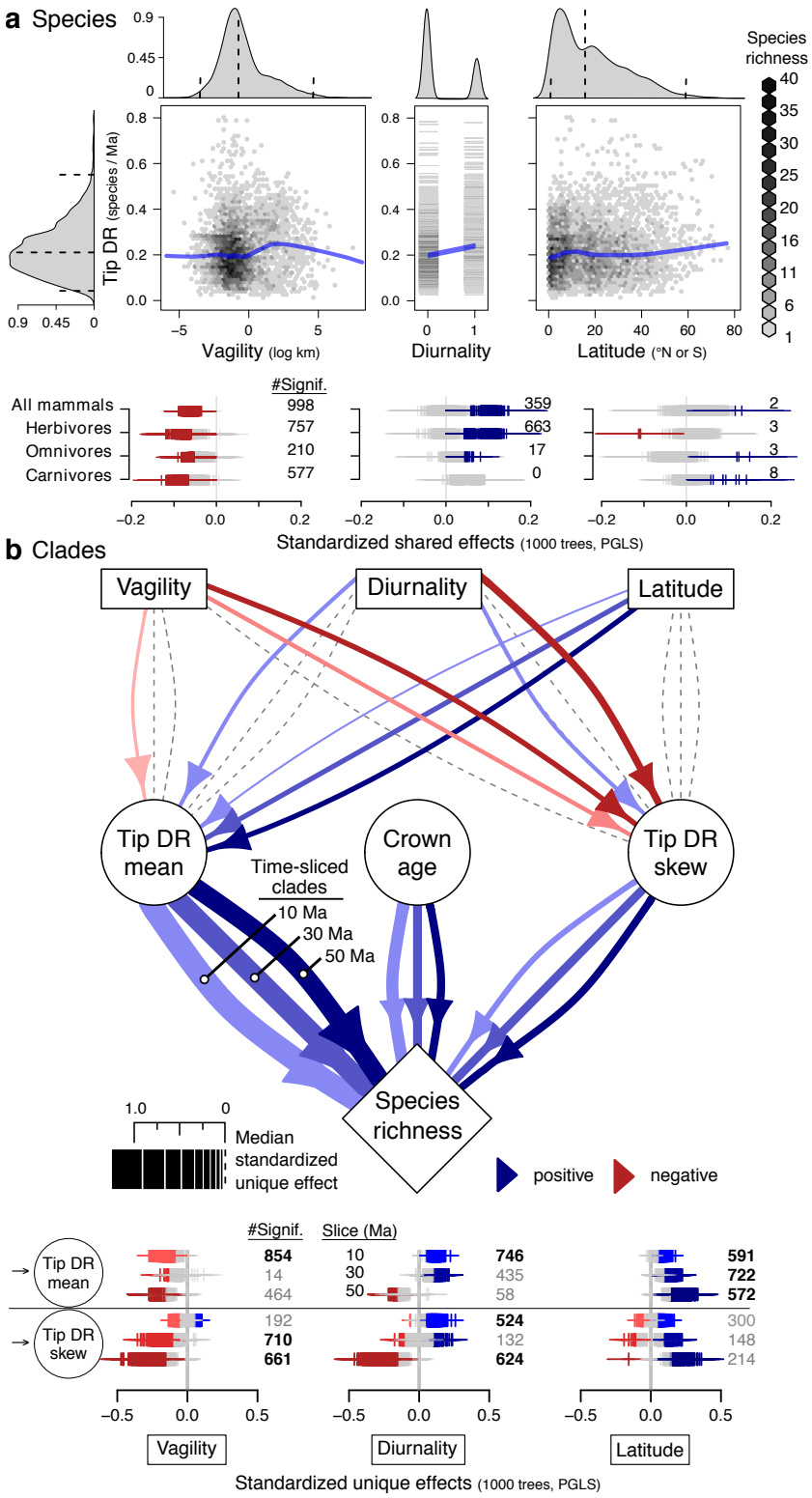

Fig. 5. Connecting clade ages, rates, richness, and traits in the mammal tree of life. (**a**, top panel) Distribution of species-level diversification rates (tip DR, mean of 10,000 trees) relative to per-species estimates of vagility (maximum natal dispersal distance), diurnality (0=nocturnal, 1=diurnal or cathemeral), and absolute value of latitude (centroid of expert range maps) across 5,675 species (excluding extinct and marine species). Loess smoothing lines visualize general trends (blue, span=0.33). Species-level effects (bottom panel) from univariate PGLS between tip DR and ecological traits subset across trophic categories (1000 trees, 95% CI, coloured if significant). (**b**) Phylogenetic path analysis of putative causal relationships between traits and rate-based processes leading to clade species richness for time-sliced clades. Path thickness, colour, and directionality denote median coefficients of model-averaged analyses. The bottom panels provide per-estimate uncertainty across analyses and time slices (slope ± SE, 1000 trees). Non-zero estimates, either positive (blue shades) or negative (red shades), are totalled in the right margin; paths present in >500 trees are bolded and displayed in path model whereas other paths have dashed lines.